Original Research

Recombinant rat CC16 protein inhibits LPS-induced MMP-9 expression via NF-κB pathway in rat tracheal epithelial cells

Min Pang[1], Hailong Wang[2], Ji-Zhong Bai[3], Dawei Cao[1], Yi Jiang[1], Caiping Zhang[1], Zhihong Liu[1], Xinri Zhang[1], Xiaoyun Hu[1], Jianying Xu[4] and Yongcheng Du[5]

[1]Department of Respiration, the First Hospital, Shanxi Medical University, Taiyuan, Shanxi 030001, China; [2]Academy of Basic Medicine, Shanxi Medical University, Taiyuan, Shanxi 030001, China; [3]Department of Physiology, Faculty of Medical and Health Sciences, University of Auckland, Auckland 1142, New Zealand; [4]Department of Respiration, Shanxi Da Yi Hospital, Taiyuan, Shanxi 030032, China; [5]Department of Respiration, the Provincial People's Hospital of Shanxi Medical University, Taiyuan, Shanxi 030012, China
Corresponding author: Yongcheng Du. Email: 1806514968@qq.com

Abstract

Clara cell protein (CC16) is a well-known anti-inflammatory protein secreted by the epithelial Clara cells of the airways. It is involved in the development of airway inflammatory diseases such as chronic obstructive pulmonary disease and asthma. Previous studies suggest that CC16 gene transfer suppresses expression of interleukin (IL)-8 in bronchial epithelial cells. However, its role in the function of these cells during inflammation is not well understood. In this study, we evaluated the effect of CC16 on the expression of matrix metalloproteinase (MMP)-9 in lipopolysaccharide (LPS)-stimulated rat tracheal epithelial cells and its underlying molecular mechanisms. We generated recombinant rat CC16 protein (rCC16) which was bioactive in inhibiting the activity of phospholipase A_2. rCC16 inhibited LPS-induced MMP-9 expression at both mRNA and protein levels in a concentration-dependent (0–2 μg/mL) manner, as demonstrated by real time RT-PCR, ELISA, and zymography assays. Gene transcription and DNA binding studies demonstrated that rCC16 suppressed LPS-induced NF-κB activation and its binding of gene promoters as identified by luciferase reporter and gel mobility shift assays, respectively. Western blotting and immunofluorescence staining analyses further revealed that rCC16 concentration dependently inhibited the effects of LPS on nuclear increase and cytosol reduction of NF-κB, on the phosphorylation and reduction of NF-κB inhibitory IκBα, and on p38 MAPK-dependent NF-κB activation by phosphorylation at Ser276 of its p65 subunit. These data indicate that inhibition of LPS-mediated NF-κB activation by rCC16 involves both translocation- and phosphorylation-dependent signaling pathways. When the tracheal epithelial cells were pretreated with chlorpromazine, an inhibitor of clathrin-mediated endocytosis, cellular uptake of rCC16 and its inhibition of LPS-induced NF-κB nuclear translocation and also MMP-9 production were significantly abolished. Taken together, our data suggest that clathrin-mediated uptake of rCC16 suppresses LPS-mediated inflammatory MMP-9 production through inactivation of NF-κB and p38 MAPK pathways in tracheal epithelial cells.

Keywords: CC16, matrix metalloproteinase 9, airways inflammation, NF-κB signaling, endocytosis, lipopolysaccharide

***Experimental Biology and Medicine* 2015; 240: 1266–1278. DOI: 10.1177/1535370215570202**

Introduction

Clara cell protein (CC16), also known as UP1, UG, PCB-BP, or CC10, is a 16-kDa homodimeric protein secreted predominantly by non-ciliated airway epithelial (Clara) cells and is regarded as an anti-inflammatory factor native to the lung.[1–3] In the lungs, CC16 suppresses the release of pro-inflammatory cytokines, such as TNF-α, IL-1β, and IFN-γ.[4] Reduced levels of CC16 in bronchial epithelium or sputum supernatants of chronic obstructive pulmonary disease (COPD) patients and reduction of CC16-positive epithelial cells in small airways of asthmatics both contribute to aggravation of inflammatory responses in chronic lung inflammation.[5–7] Gene knockout studies show that mice which lack CC16 develop increased susceptibility and exaggerated inflammatory responses to the exposure of hyperoxic and infectious agents.[8] These results indicate that CC16 is important in maintaining lung homeostasis.

In lung inflammation diseases, lung structures are mainly damaged by excessive proteinase activity, such as matrix metalloproteinase 9 (MMP-9).[9] MMP-9 is the largest and most structurally complex member of the MMPs which

degrade extracellular matrix and cellular junctions during inflammatory cell recruitment.[10–12] Increased levels of MMP-9 have been found in the sputum and lavage samples of patients during COPD and asthma exacerbation.[13,14] Elevated MMP-9 expression in the lung diseases is also associated with activation of nuclear factor kappa B (NF-κB),[15,16] which is a principal transcription factor involved in the process of airway inflammation.[17] Therefore, a combination of CC16 deficiency in chronic lung inflammation, together with advancing lung damages due to increase in MMP-9, suggests that CC16 mediates MMP-9 expression and contributes to lung homeostasis.

The aim of this study was to test the hypothesis that CC16 suppresses inflammatory response by reducing MMP-9 expression through NF-κB signaling pathways. We generated recombinant rat CC16 (rCC16) to treat rat tracheal epithelial cells (RTE) and monitored the inflammatory responses (i.e. MMP-9 expression and NF-κB activation) induced by subsequent LPS incubation.[18,19] MMP-9 expression was determined by real time RT-PCR, ELISA, and its potential activity using zymography assays. NF-κB activation was followed by luciferase reporter, electrophoretic mobility shift assay (EMSA) and Western blotting techniques, and NF-κB binding of gene promoters by gel mobility shift assays. We also explored the cellular entry pathway of rCC16 by clathrin-mediated endocytosis. Our results suggest that administration of rCC16 reduces LPS-induced MMP-9 expression and activation of NF-κB pathways in RTE cells.

Materials and methods

Expression and purification of recombinant rCC16 protein

rCC16 was expressed and purified as described previously.[20] Briefly, the open reading frame (ORF) of rat CC16 gene (GeneBank Accession Number: NM_013051) was amplified from rat lung cDNA library (provided by Min Guo, Shanxi Medical University) and cloned into the pET-30a (+) vector (Novagen, Germany). His-tagged rCC16 was induced to express in *Escherichia coli* Rosetta (DE3) cells with 0.1 mM isopropy-β-D-thiogalactoside (IPTG) at 23°C and purified via Ni^{2+}-NTA agarose (Qiagen, Germany) by elution with 150 mM imidazole at 4°C. The endotoxin contents in the protein preparations were determined and removed by using a chromogenic end-point endotoxin assay Kit and a ToxinEraser™ endotoxin removal kit according to the manufacturer's instructions (Horseshoe Crab Reagent Manufactory, Xiamen, China). Less than 0.1 EU/mL of endotoxin was detected in the final purified proteins. Purity of rCC16 was analyzed using a ÄKtA avant 25 high-performance liquid chromatography (HPLC) system (Zorbax SB-C18, Agilant, USA) according to previous protocols,[21,22] and protein contents were monitored by UV detection at 280 nm/254 nm/214 nm. Over 95% purity, rCC16 was quantified using Bicinchoninic Acid assay Protein Reagent kit (CWBIO, Beijing, China), dialyzed against PBS, filtered through a 0.2 μm pore membrane, and stored at –70°C until use.

Cell culture and drug treatments

The rat tracheal epithelial (RTE) cell line was purchased from the Cell Culture Center of the Chinese Academy of Medical Sciences (Beijing, China) and cultured in Minimal Essential Medium with Earle's Salts (MEM-EBSS, Life Technologies) supplemented with 20% fetal calf serum (HyClone; Thermo Scientific), 100 U/mL penicillin, and 100 μg/mL streptomycin in a 5% CO_2 humidified atmosphere at 37°C. A549 cells were kindly provided by Dr Junbo Liang (National Laboratory of Medical Molecular Biology, Institute of Basic Medical Sciences, Chinese Academy of Medical Sciences, Peking Union Medical College, Tsinghua University) and cultured in Dulbecco's Modified Eagle Medium (Life Technologies) supplemented with 10% fetal calf serum. Adherent cells were passaged every 3–4 days with 0.25% trypsin–EDTA (Life Technologies).

Cell Counting Kit-8 (CCK-8, Dojindo, Japan) and Trypan Blue (Fluka, USA) exclusion methods were used for cell viability assays. RTE cells were seeded in 96-well plates at 1×10^4 cells/well in triplicate and cultured with rCC16 at 5, 10, 20 μg/mL or PBS controls for one, three, five, or seven days. The cells were then incubated with 100 μL of fresh medium containing 10 μL CCK-8 reagent at 37°C for 3 h, and colorimetric CCK-8 reduction by live cells was measured at 450 nm with an ELISA plate reader. For Trypan Blue exclusion assay, RTE cells were seeded at 1×10^5 cells/well in 24-well plates in triplicate and treated as earlier. After trypsinization, the cells were stained with Trypan Blue (0.4%), and the number of viable (non-stained) and dead (stained) cells was determined using a hemocytometer under a phase-contrast microscopy.

For drug treatment, subconfluent cultures of RTE cells were washed with PBS, incubated with rCC16 at 0.5, 1.0, or 2.0 μg/mL in serum-free media for 2 h prior to LPS (0.1 μg/mL) application, and were maintained for further 1, 24 h. For NF-κB pathway analysis, pyrrolidine dithiocarbamate (PDTC, Sigma-Aldrich) was added to the RTE cells in complete media at 50 μM 2 h prior to the LPS treatment in serum-free media for further 24 h. Cell culture supernatants or cells were then harvested for subsequent analysis as described below.

Phospholipase A_2 (PLA_2) activity assay

The activity of PLA_2 was measured using lecithin as a substrate by acid–base titrations according to previous protocols[23,24] with minor modifications. In the presence of Ca^{2+}, lecithin is hydrolyzed by PLA_2 into titratable fatty acids. Briefly, the reaction was performed at 37°C for 60 min in 10 mL of a reaction medium containing 1.2 nM PLA_2, 10 mM $CaCl_2$, 3 mM lecithin (Sigma) substrate solution (incl. 80 mM glycine, 3 mM boric acid, 4.8 mM sodium deoxycholate, pH 8.50) in presence or absence of rCC16 at various concentrations. The reaction was terminated by adding EDTA at 1.5 mM to the testing tubes, and the same amount of EDTA was included in the reference tubes (containing the same concentration of rCC16) in the absence of $CaCl_2$ before the incubation. The pH in the reference tubes was determined to the equivalent of their

testing tubes with a Starter 2100 pH meter (Ohaus, USA) using 2 mM HCI as titrant. In each experiment, controls were included which were not exposed to rCC16. PLA_2 activity was quantified in absolute units by the consumption of nanomoles of HCI per min required to match the fatty acids produced in the testing, and results were expressed as % of tests relative to controls without rCC16.

RT-PCR

After treatment with rCC16 and LPS, cells were harvested and total RNA was extracted using Trizol reagent (CWBIO, Beijing, China). The concentration and purity of RNA were quantified by ultraviolet absorbance at 260 and 280 nm. Real-time RT-PCR was performed with the Applied Biosystems® Real-Time PCR Instruments using an UltraSYBR Two Step RT-qPCR Kit (CWBIO, Beijing, China) according to the manufacturer's instructions. Reverse transcription was performed for 50 min at 42°C with 1 μg total RNA. PCR was carried out in a 20 μL reaction mixture containing 1 μL cDNA template under conditions: denaturing at 95°C for 1 min, 40 cycle amplification at 95°C for 10 s and 60°C for 40 s in triplicates. The $2^{-\Delta\Delta CT}$ method was used to calculate the relative levels of gene expression, and glyceraldehyde-3-phosphate dehydrogenase (GAPDH) expression was used as internal control. The sequences of primers used for the real-time PCR were: MMP-9 (sense 5′-TATCACTACCACGAGGACTCCC-3′, antisense 5′-TCAGGTT TAGAGCCACGACC-3′) and GAPDH (sense 5′-GTGCCAGCCTCGTCTCATAG -3′, antisense 5′-CTTTGTCACAAGAGAAGGCAG-3′). To detect endogenous CC16 mRNA expression in RTE cells, total RNA was extracted from RTE cells using Trizol reagent, cDNA was synthesized, and CC16 was amplified according to the published protocols.[20] GAPDH was used as an internal control with the primers: sense 5′-ACCACAGTCCATGCCATCAC-3′, antisense 5′-TCC ACCACCCTGTTG CTGTA-3′.

Quantification of MMP-9 protein levels in culture supernatants

RTE cells, seeded at 2.5×10^5 cells/well in 12 well plates, were cultured overnight, incubated with or without rCC16 at different concentrations for 2 h, and then followed by LPS stimulation at 0.1 μg/mL in serum-free media for the time as indicated. Culture supernatants were harvested, centrifuged, and used for determining the levels of MMP-9. For assessing the role of endocytosis, cells were treated with 30 μM chlorpromazine (Sigma) or vehicles for 30 min, incubated with or without 2.0 μg/mL rCC16, and then followed by LPS stimulation at 0.1 μg/mL for 24 h. Culture supernatants were harvested, centrifuged, and used for determining the levels of MMP-9 using a rat MMP-9 ELISA development kit (Westang, Shanghai, China) according to the manufacturer's instructions. The sensitivity of this kit was 2.0 ng/mL.

Gelatin zymography analysis of MMP-9

Following the treatments with rCC16 for 2 h and LPS for further 24 h as described earlier, the potential enzyme activities of MMP-9 in the cell culture supernatants were determined with gelatin zymography assay as a measure of its levels of expression. Protein content was determined with the BCA method, and 20 μg proteins were fractionated by 10% SDS-PAGE containing 1 mg/mL gelatin A (Sigma) that serves as the enzyme substrate. After electrophoresis, the gel was soaked to remove SDS in a Triton X-100 solution (zymograming), the proenzyme of MMP-9 in the gel is activated to react with its gelatin substrate. Following staining with 0.5% Coomassie Blue R-250 for 30 min and destaining with 45% methanol, 10% (v/v) acetic acid, the clear bands generated due to MMP-9 activities against a blue background were quantified by densitometry using Tanon 1600 Gel Image Analysis System (Tanon, Shanghai, China).

NF-κB luciferase reporter assay

RTE cells seeded at 1×10^5 cells/well in 24 well plates were cultured overnight and co-transfected at 70–80% confluence with 0.5 μg NF-κB promoter Firefly luciferase reporter and 0.02 μg Renilla luciferase constructs (Beyotime, China) using Lipofectamine 2000 (Life Technologies) according to the manufacturer's protocols. Twenty-four hours after transfection, the cells were exposed to rCC16 at different concentrations for 2 h and then incubated with 0.1 μg/mL LPS for another 24 h. Cell extracts were prepared and the activities of the two reporter enzymes (Firefly and Renilla luciferases) were determined using the Dual-Luciferase Reporter Assay System (Promega) with a luminometer (TD-20/20, Turner BioSystems, USA) as per the manufacturer's instructions. The transcriptional activities of NF-κB were expressed as relative luciferase activities calculated as the ratio of Firefly luciferase activity to Renilla luciferase activity.

Electrophoresis mobility shift assay

Nuclear proteins were extracted from RTE cells treated with rCC16 (1.0 or 2.0 μg/mL, 2 h) and LPS (0.1 μg/mL, 1 h) and incubated with biotin-labeled double stranded oligonucleotide containing the consensus sequence of NF-κB-DNA binding site (59-AGTTGAGGGGACTTTCCCAGG-39) as described.[18] Binding reaction mixtures (20 μL) containing 4 μg nuclear extract protein, 1 μg poly-dI.dC (Thermo Scientific), and 20 ficomoles biotin-labeled probe in binding buffer (10 mM Tris, 50 mM potassium chloride, 1 mM dithiothreitol, 0.1 mM EDTA, 2.5% glycerol, 5 mM magnesium chloride) were incubated for 20 min at room temperature. Cold competition and non-specific binding was performed by adding 200-fold excess of unlabeled probe to the reaction mixtures for 20 min prior to addition of biotinylated probes. DNA–protein complexes were resolved on a 6% non-denaturing polyacrylamide gels and blotted onto a Biodyne B (0.45 μm) positively charged nylon membrane (Thermo Scientific). The retarded bands were detected by chemiluminescence using the LightShift Chemiluminescent EMSA kit according to the manufacturer's instructions (Thermo Scientific).

Western blotting analysis

Total protein extraction was prepared by cell lysing using SDS lysis buffer containing 50 mM Tris–HCl (pH 6.8), 10% glycerol, and 2% SDS. Nuclear proteins were extracted by using a NE-PER Nuclear and Cytoplasmic Extraction kit (Thermo Scientific). The protein samples were quantified using the BCA protein assay reagent, resolved by 12% SDS–PAGE gel electrophoresis and transferred to polyvinylidene fluoride (PVDF) membranes. Membranes were blocked for 1 h at room temperature with 5% skim milk and then incubated overnight at 4°C with the indicated primary antibodies at 1:1000 dilutions unless otherwise indicated: p65, IκBα, Phospho-IκBα (Ser32), p38 MAPK, Phospho-p38 MAPK (Thr180/Tyr182) (Cell Signaling Technology), Phospho-p65 (Ser276), Histone H1, CC16 (Santa Cruz), or β-actin (1:3000, Sigma). Proteins were visualized using an anti-rabbit, anti-mouse, or anti-goat secondary antibody conjugated to Horseradish Peroxidase (HRP) and a chemiluminescence ECL detection system (Pierce, USA). Band intensities were quantified using a Tanon 1600 Gel Image Analysis System.

Immunofluorescence staining assay

Subconfluent RTE cells grown on glass coverslips were incubated with or without rCC16 at different concentrations for 2 h and then subjected to LPS stimulation at 0.1 μg/mL for another 1 h. The subcellular distributions of NF-κB/p65 were assessed by immunofluorescence staining. To verify the mode of cellular uptake of rCC16, RTE cells grown on coverslips in 12-well plates were exposed to 30 μM chlorpromazine (Sigma) or controls for 30 min at 37°C in serum-free medium. For assays to determine the effect of chlorpromazine on rCC16 activities, the RTE cells treated with chlorpromazine and rCC16 were subjected to incubations with LPS at 0.1 μg/mL for another 1 h. The culture medium was replaced with growth medium containing 2.0 μg/mL rCC16 and incubated for another 30 min. The subcellular locations of His-rCC16 were analyzed via immunofluorescence staining. To detect–CC16 expression in RTE cells, subconfluent RTE cells and A549 cells (which expresses CC16[25] and serves as a positive control) were cultured on glass coverslips for 24 h. The cells were fixed with 4% paraformaldehyde in PBS for 20 min at RT, blocked with 3% bovine serum albumin in PBS, and incubated overnight at 4°C with a rabbit anti-p65 antibody (1:100, Cell Signaling Technology) or a mouse anti-His monoclonal antibody (1:100, Cell Signaling Technology) for the detection of His-tagged rCC16 using a mouse IgG isotype as negative controls. A goat anti-CC16 polyclonal antibody (1:50) was used for the detection of endogenous CC16 with a goat IgG isotype as negative controls. Following washes with PBS, cells were stained with an Alexa Fluor 488-conjugated goat anti-rabbit antibody (1:200), Alexa Fluor 546-conjugated goat anti-mouse antibody (1:400), or Alexa Fluor 546 donkey anti-goat antibody (1:400) (Life Technologies) and nuclei staining with DAPI (Sigma) in PBS for 1 h at RT. Cells were visualized and imaged under a fluorescence microscope (Olympus, CKX41-F32FL).

Statistical analysis

All data are presented as mean ± SD for three or more independent experiments. Multiple group comparisons were performed with one-way analysis of variance, and comparisons between two groups were performed by the Student's *t*-test by using the Prism software (Version 5, GraphPad). Differences were considered statistically significant at a P value less than 0.05.

Results

rCC16 inhibits the activity of PLA_2

In order to assess the role of rCC16 in suppression of LPS-induced inflammatory responses, we first generated rCC16 and determined its bioactivity and concentration range of cytotoxicity. His-tagged rCC16 was expressed in *E. coli* cells and purified via Ni^{2+} gel column, the purity was over 95% as detected by SDS-PAGE with Coomassie blue R250 staining[20] and by high performance liquid chromatography (HPLC) as shown in supplemental Figure 1. For all other experiments, we employed the RTE cell line in which CC16 expression is absent or at very low levels as determined by RT-PCR, Western blotting, and immunofluorescence staining assays (supplemental Figure 2). To evaluate the

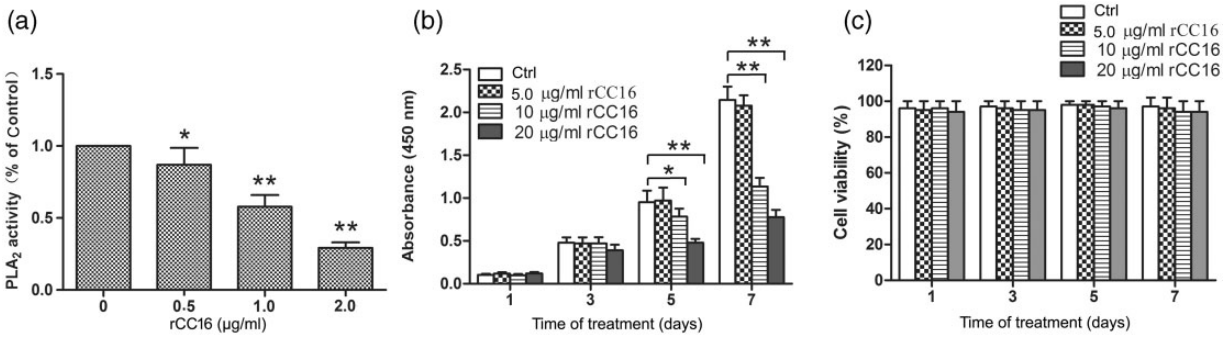

Figure 1 Effects of rCC16 protein on PLA2 activity and RTE cell viability. (a) Acid–base titration analysis shows concentration-dependent inhibition of PLA_2 activity by rCC16. (b) Colorimetric CCK-8 reduction assays show time-dependent response of rCC16 on RTE cells proliferation. Data are presented as mean ± SD (n = 3) of three independent experiments. *$p < 0.05$ and ** $p < 0.01$ relative to vesicle controls. (c) Trypan blue exclusion assay demonstrates RTE cell viability following rCC16 treatment as stated in (b). Results are expressed as percentage of trypan blue exclusive viable cells relative to total number of cells. Data are presented as mean ± SD (n = 3) of three independent experiments

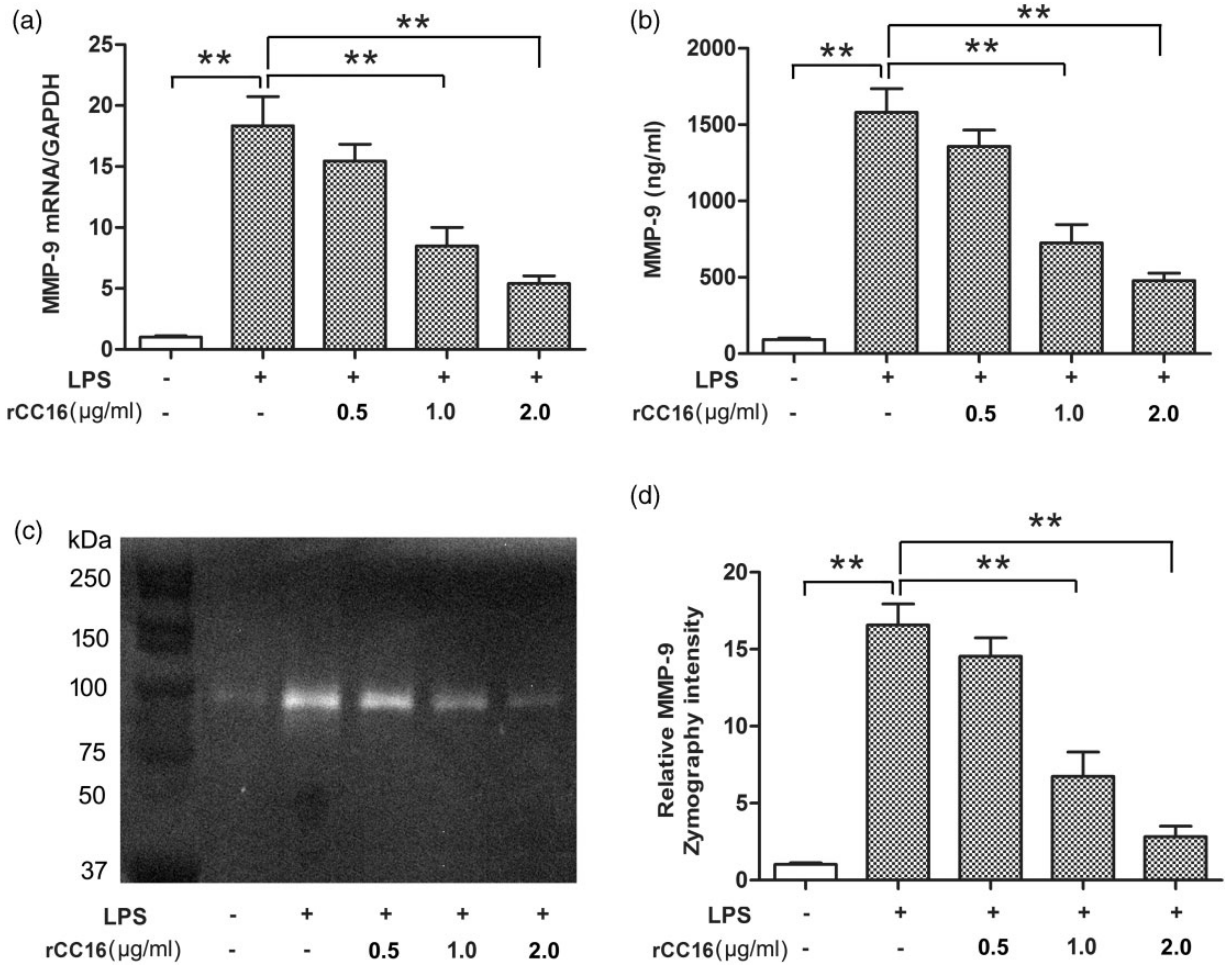

Figure 2 rCC16 inhibits LPS-stimulated MMP-9 expression in RTE cells. (a) Real-time PCR and (b) ELISA assays show inhibition of LPS-stimulated MMP-9 expression by rCC16 in a concentration-dependent manner. RTE cells were incubated with rCC16 (0–2.0 μg/mL for 2 h prior to LPS exposure at 0.1 μg/mL for further 24 h. For qPCR determinations, results are expressed as ratios of $2^{-\Delta\Delta CT}$ qPCR values for MMP-9 mRNA/GAPDH. For ELISA determinations, results are expressed as absolute protein values of MMP-9. (c) Gelatin zymography assay and (d) quantitative analysis of MMP-9 activity in cell culture media obtained as described in (c). Data are presented as mean ± SD (n = 3) of three independent experiments. $^{**}p < 0.01$ indicates significant difference between groups as shown

biological activity of rCC16, we initially determined the effect of rCC16 on PLA_2 activity since endogenous CC16 protein inhibits PLA_2 activity.[26,27] Figure 1(a) shows that rCC16 inhibited PLA_2 activity in a concentration-dependent manner. After 1 h treatment, significant PLA_2 inhibition was observed at 0.5 μg/mL rCC16 ($P<0.05$) and reached higher level at 1.0 and 2.0 μg/mL rCC16 ($P<0.01$).

To analyze the cytotoxic effect of rCC16 on its applications, RTE cells were treated with rCC16 at 5, 10, 20 μg/mL or PBS control, and cell viability was assessed one, three, five, and seven days later. As shown in Figure 1(b), exposure of RTE cells to rCC16 evoked both concentration- and time-dependent inhibition of cell proliferation compared to PBS controls, as determined by CCK-8 assays. While significant cell proliferations were observed in PBS controls and cells treated with 5 μg/mL rCC16 for seven days, significant reductions of cell numbers were also observed at 10 and 20 μg/mL after five days exposure to rCC16 and reached higher level at day 7 ($P < 0.01$). To further verify that the cell number reduction seen at high concentrations of rCC16 over five days is due to reduced cell proliferation, we performed trypan blue staining of the cells and counted the living and dead cells under phase contrast microscopy. Indeed, no difference of cell viability was observed in cells treated with different concentrations of rCC16 over the seven days (Figure 1(c)). These data indicated that the rCC16 we produced was biologically active and displayed no cytotoxic effect at low concentrations (5 μg/mL or lower).

rCC16 inhibits LPS-induced MMP-9 expression in RTE cells

LPS is a major component of the outer membrane of gram-negative bacteria and commonly used to study inflammation.[28] To evoke inflammatory responses in the RTE cells, we used LPS at a concentration of 0.1 μg/mL which was previously shown to induce MMP9 mRNA expression through the NF-κB pathway in A549 lung epithelial cells.[29] A role of MMP-9 in the development of inflammation is also well established as an inflammatory marker.[30,31] To determine whether rCC16 plays an anti-inflammation

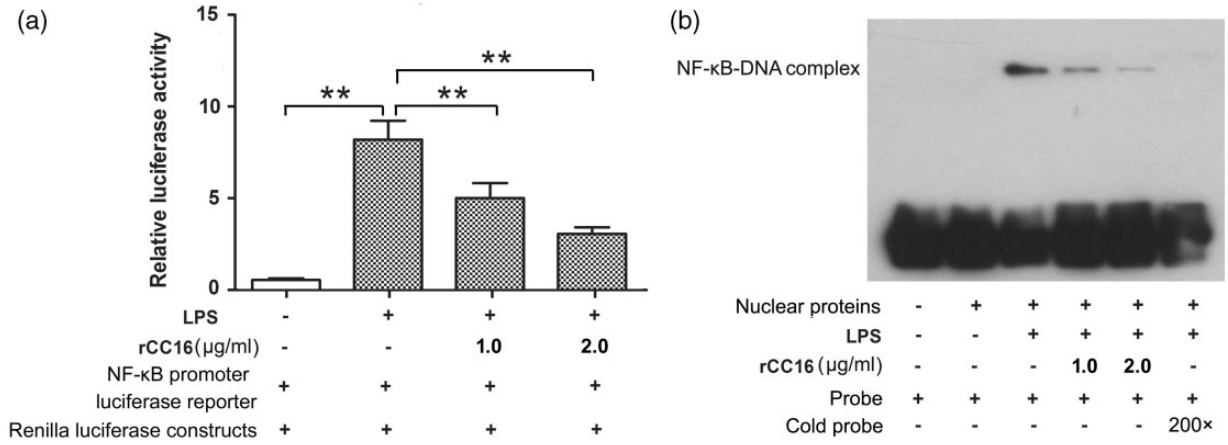

Figure 3 rCC16 suppresses LPS-induced activation and DNA binding of NF-κB transcription factors in RTE cells. (a) Luciferase reporter assay and (b) EMSA show concentration-dependent inhibition of the transcriptional activity (a) and DNA-binding (b) of a NF-κB-responding promoter construct by rCC16 in RTE cells stimulated with 0.1 μg/mL LPS for 24 h (luciferase reporter assay) or 1 h (EMSA assay). Specific NF-κB binding was assessed using a competitive binding between biotin-labeled NF-κB oligonucleotide and 200-fold excess of its non-labeled equivalent. Data are presented as mean ± SD (n = 3) of three independent experiments. $^{**}p < 0.01$ indicates significant difference between groups as shown

role in airway epithelial cells, we therefore investigated the effect of rCC16 on LPS-induced MMP-9 expression in RTE cells by real-time PCR and ELISA assays. RTE cells were pretreated with rCC16 at 0.5, 1.0, and 2.0 μg/mL for 2 h prior to the addition of 0.1 μg/mL LPS for further 24 h. As shown in Figure 2, increased expression of MMP-9 was observed on both mRNA (Figure 2(a)) and protein levels (Figure 2(b)) in LPS-treated RTE cells, and these LPS-stimulated MMP-9 expressions were inhibited by rCC16 in a dose-dependent manner, being significant at concentrations over 1.0 μg/mL. In accord, a similar concentration-dependent reduction of MMP-9 activities in the culture media of rCC16-treated RTE cells was revealed by zymography assays (Figure 2(c) and (d)). These results suggest that rCC16 inhibits LPS-induced MMP-9 expression and its activities.

rCC16 suppresses the transcriptional activity and DNA binding of NF-κB

NF-κB activation is critical to LPS-induced transcriptional regulation of inflammation[32] and MMP-9 activities in airway inflammation.[16] To determine whether the NF-κB pathway is required for MMP9 expression in the RTE cells we employed here, the specific NF-κB inhibitor PDTC (50 μM) was applied to the cells for 2 h prior to LPS treatment. The results showed that PDTC significantly inhibited LPS-evoked MMP9 protein expression (supplemental Figure 3), as previously determined under similar conditions in the lung epithelial cells.[29] We next performed dual luciferase reporter assays to assess whether suppression of MMP-9 by rCC16 in LPS-stimulated RTE cells is dependent on NF-κB-mediated transcriptional activation. As shown in Figure 3(a), LPS caused an approximate ninefold increase in relative luciferase activity, and rCC16 inhibited LPS-induced NF-κB transcriptional activity in a concentration-dependent manner, from 38.8% at 1.0 μg/mL to 62.6% reduction at 2.0 μg/mL. To further verify the inhibitory effect of rCC16 on NF-κB activity, EMSA were employed to determine whether rCC16 could inhibit DNA binding activity of NF-κB using a biotin-labeled consensus p65 probe of NF-κB. As shown in Figure 3(b), LPS treatment augmented the DNA binding activity significantly, and rCC16 suppressed LPS-induced NF-κB-DNA binding at 1.0 and 2.0 μg/mL in a concentration-dependent manner. These findings indicate that rCC16 suppresses the transcriptional activity of NF-κB by blocking its DNA bindings.

rCC16 suppresses NF-κB nuclear translocation

In resting cells, NF-κB is sequestered in the cytosol by its inhibitor IκB. Once it is stimulated by LPS, IκBα is phosphorylated and rapidly degraded via proteasome pathway, leading to the release of NF-κB and its translocation to the nucleus.[30,33] We therefore performed Western blotting analysis to assess the effect of rCC16 on the cytoplasmic and nuclear distribution of the NF-κB proteins upon LPS stimulation. As shown in Figure 4(a), an increased level of NF-κB/p65 in the nucleus was seen in LPS-treated cells, and this nuclear increase of NF-κB/p65 protein was significantly suppressed by rCC16 at 1.0 and 2.0 μg/mL but not 0.5 μg/mL. Being consistent, decreased level of cytosol NF-κB/p65 was observed in LPS-treated cells, and rCC16 rescued this decrease at similar concentrations (Figure 4(b)) without affecting the total cellular levels of NF-κB/p65 (Figure 4(c)). To further confirm the effect of CC16 on the relocation of NF-κB in LPS-treated RTE, we performed immunofluorescence staining of NF-κB. Distribution of NF-κB/p65 was found in the nucleus in LPS-treated cells, and it was significantly repressed by rCC16 at concentrations 1.0 and 2.0 μg/mL but not 0.5 μg/mL (Figure 4(d)). These data suggest that rCC16 inhibition of NF-κB transcriptional activity also involves blockage of LPS-induced nuclear translocation of its p65 subunit in the RTE cells.

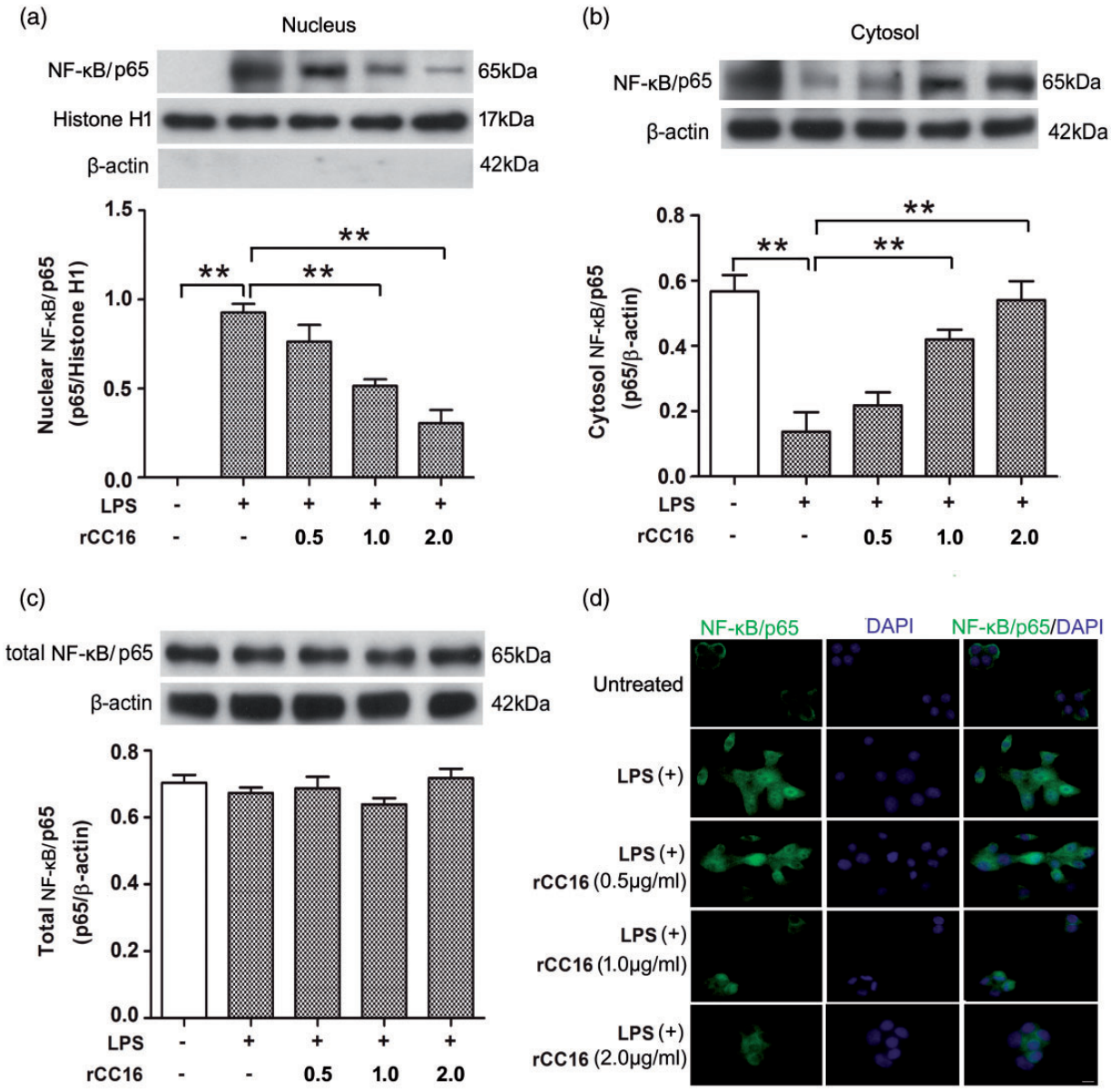

Figure 4 rCC16 prevents LPS-induced NF-κB nuclear translocation in RTE cells. RTE cells were treated with rCC16 at indicated concentrations for 2 h prior LPS exposure at 0.1 μg/mL for another 1 h. Subcellular distributions of NF-κB/p65 were determined by Western blotting analysis in nuclear (a) and cytoplasm (b) preparations together with total level of NF-κB/p65 (c). Potential contamination of the nucleus fractions by cytosol fractions was checked and excluded by Western blotting with the β-actin antibody in the same samples in (a). One representative of three independent experiments is shown, and data are presented as the mean ± SD (n = 3) of three independent experiments. $^{**}p < 0.01$ indicates significant difference between groups as shown. (d) Immunofluorescence staining of NF-κB/p65 (green) and nuclei with DAPI (blue) was conducted to verify the effect of CC16 on the subcellular distributions of NF-κB in RTE cells with various treatments as indicated. Scale bar, 100 μm. (A color version of this figure is available in the online journal.)

rCC16 prevents the phosphorylation of IκBα

As mentioned earlier, NF-κB activity is regulated by cytoplasmic phosphorylation and degradation of its inhibitory unit IκB, and translocation of its p65 subunit to the nucleus.[30,34] To determine whether rCC16 inhibition of NF-κB nuclear translocation also involves IκBα, cellular phosphorylation and degradation of IκBα upon LPS stimulation and rCC16 pretreatment were determined by immunoblot analysis. We found that LPS exposure resulted in increased phosphorylation of IκBα and that pretreatment of cells with rCC16 suppressed this phosphorylation at concentrations 1.0 μg/mL and above (Figure 5(a)). In accord, the decrease in the cellular level of IκBα caused by LPS was attenuated by rCC16 pretreatment at similar concentrations (Figure 5(b)). These results indicate that rCC16 treatment of the RTE cells also prevents LPS-induced phosphorylation and degradation of IκBα and subsequent activation of NF-κB.

rCC16 inhibits LPS-induced phosphorylation of NF-κB/p65 and p38 MAPK

Since NF-κB activation is regulated by either its translocation- or phosphorylation-dependent pathways,[30,34] we also

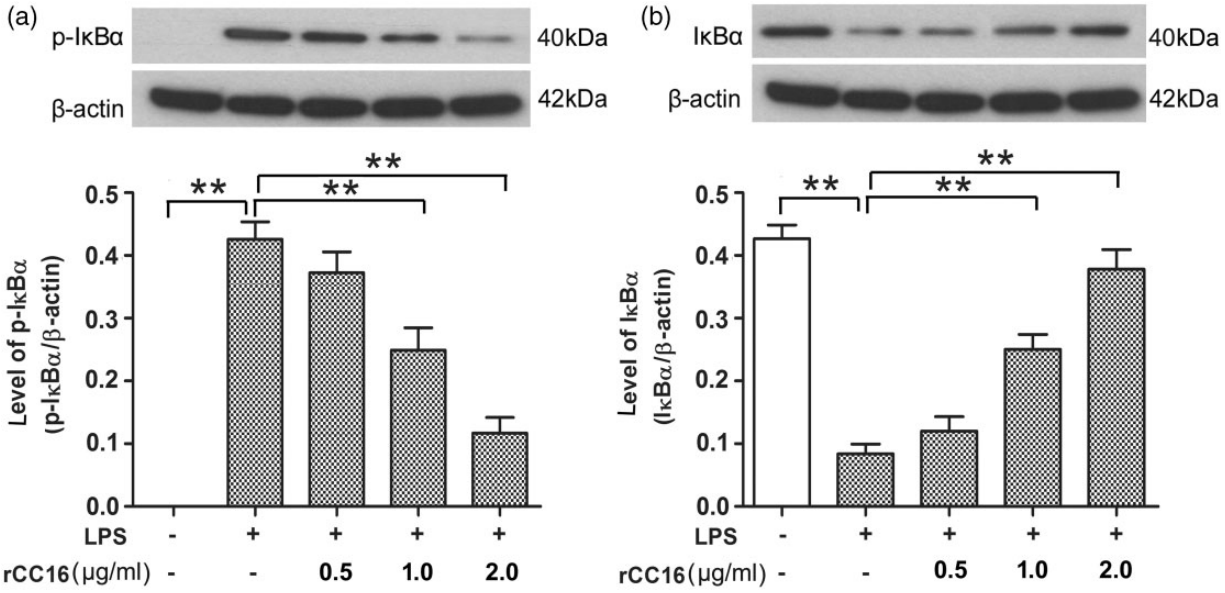

Figure 5 rCC16 inhibits LPS-induced phosphorylation and degradation of IκBα in RTE cells. RTE cells were treated with rCC16 at indicated concentrations for 2 h prior LPS exposure at 0.1 μg/mL for another 1 h. Total proteins were extracted and the levels of phosphorylated IκBα (a) and IκBα (b) relative to β-actin were detected by Western blotting. One representative of three independent experiments is shown. Data are presented as the mean ± SD (n = 3) of three independent experiments. $^{**}p < 0.01$ indicates significant difference between groups as shown

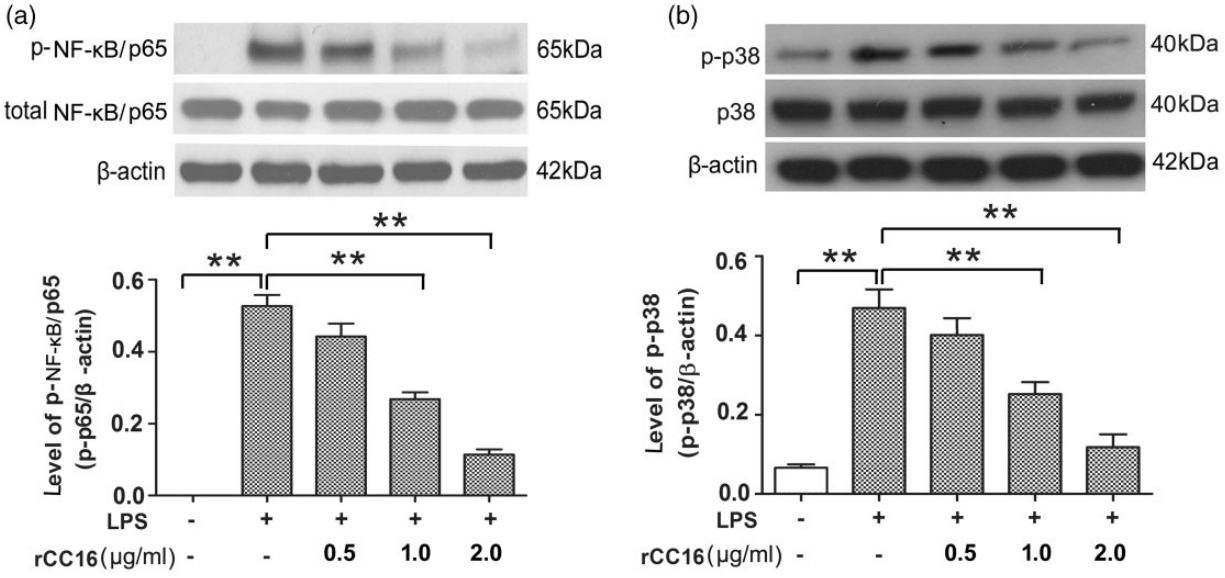

Figure 6 rCC16 inhibits LPS-induced phosphorylation of NF-κB/p65 and p38 MAPK. RTE cells were treated with rCC16 at indicated concentrations for 2 h prior LPS exposure at 0.1 μg/mL for another 1 h. Total proteins were extracted, and the levels of phosphorylated p65 (a) and p38 MAPK (b) were detected by Western blotting. One representative of three independent experiments is shown. Data are presented as the mean ± SD (n = 3) of three independent experiments. $^{**}p < 0.01$ indicates significant difference between groups as shown

measured the phosphorylation of p65 NF-κB. As shown in Figure 6(a), LPS increased the phosphorylation of p65 at ser276, pretreatment of cells with rCC16 suppressed this phosphorylation in a concentration-dependent manner without affecting the total levels of p65. It has been reported that the phosphorylation of p65 at Ser276 is associated with p38 MAPK signaling pathways.[35] We therefore investigated whether the inhibition of inflammatory response by rCC16 also involves p38 MAPK. As shown in Figure 6(b), LPS (0.1 μg/mL) significantly increased the level of p-p38 compared to untreated controls, and this LPS-induced p-p38 increase was reduced by rCC16 at concentrations 1.0 μg/mL and above. These findings indicate that rCC16 suppression of LPS-induced NF-κB activation is associated with NF-κB phosphorylation and p38 MAPK signaling pathways.

Uptake of rCC16 into RTE cells depends on clathrin-mediated endocytosis

Endocytosis is known to be involved in a variety of cellular processes[36] and is either mediated by clathrin-coated pits or by clathrin-independent mechanisms. Clathrin is a coat protein which is involved in forming specific endocytotic vesicles and mediates the internalization of a wide range of small molecules.[37] To determine whether clathrin-mediated endocytosis is involved in rCC16 signaling, we tested chlorpromazine, a drug that prevents formation of clathrin-coated pits at the plasma membrane,[38] on the uptake of rCC16 by RTE cells. As illustrated in Figure 7(a), RTE cells preincubated with chlorpromazine at 30 μM for 30 min displayed strong resistance against endocytosis of rCC16 (His-tagged) as shown by immunofluorescence staining with anti-His antibodies. To further confirm the importance of clathrin in the cellular uptake of rCC16, we determined the effect of chlorpromazine on nuclear translocation of NF-κB/p65 in rCC16-exposed and LPS-stimulated RTE cells using immunoblot analysis and immunofluorescence staining with the NF-κB/p65 antibody. Pretreatment of RTE cells with chlorpromazine (30 μM, 30 min) significantly blocked the inhibitory roles of rCC16 on LPS-induced NF-κB/p65 nuclear translocation (Figure 7(b)). In accord, chlorpromazine rescued the nuclear NF-κB/p65 distribution in presence of rCC16 and LPS (Figure 7(c)). While rCC16 was found to inhibit the translocation of NF-κB/p65 into nucleus in the presence of LPS, chlorpromazine significantly blocked the inhibitory effects of rCC16 and restored the nuclear distribution of NF-κB/p65 (Figure 7(d)). When the levels of MMP-9 in these cells were determined using ELISA analysis, increased MMP-9 productions were visualized from chlorpromazine-pretreated RTE cells which were exposed to rCC16 and LPS, suggesting that chlorpromazine abolished the inhibitory effect of rCC16 on LPS-stimulated expression of MMP-9 (Figure 7(e)). Taken together, these data demonstrate that clathrin-mediated endocytosis of rCC16 is critical for its inhibitory role in LPS-induced MMP-9 production during inflammatory responses.

Discussion

Our studies show that rCC16 suppresses LPS-induced MMP-9 expression in RTE cells, and that this effect involves NF-κB activation through phosphorylation and degradation of its inhibitor IκBα and the p38 MAPK signaling pathways. The inhibitory effects of rCC16 were abolished by blocking clathrin-mediated endocytosis. These data indicate that clathrin-mediated cellular uptake of rCC16 inhibits activation of NF-κB and MMP-9 expression during LPS-induced inflammatory responses in epithelial cells of the airways.

CC16 is a secretory protein with anti-inflammatory and immunomodulatory characteristics.[39] A decreased level of CC16 found in the bronchoalveolar lavage fluid of lungs is thought to be the contributing factor to airway inflammations.[40–43] In animal model studies, CC16 knockout-mice express exaggerated eosinophilic inflammation during allergen challenge in their lungs.[44] These studies indicate that reduced CC16 anti-inflammatory action may contribute to the induction and development of airway inflammatory diseases. To prove a role of CC16 in anti-inflammation, we generated rCC16[20] and determined its bioactivities in cultured RTE cells. We verified that our rCC16 preparations being biologically active to suppress PLA_2 activities[26,27] at concentrations (from 0.5 to 2.0 μg/mL) without causing the RTE cells to proliferate or die (Figure 1).

MMP-9 generated within the lung environment regulates many physiological processes during infection, inflammation, and subsequent tissue repairs. Elevated levels of MMP-9 have been established in COPD during the development of chronic inflammation[45,46] and are used as a distal biomarker for inflammation.[31,47] Innate immune cells including macrophages and neutrophils are the major source of MMP-9.[14,48] Infected bronchial epithelial cells also release MMP-9 in COPD patients.[49] In accord, LPS induces expression of MMP[19] and exacerbations of COPD.[50,51] In A549 lung epithelial cell cultures, LPS induces MMP-9 expression through the NF-κB pathway at 0.1 μg/mL concentration.[29] We therefore employed LPS at this concentration to determine its effect on MMP-9 expression in RTE cells and the effectiveness of rCC16 as an anti-inflammative *in vitro*. Our data suggest that LPS indeed promoted MMP-9 expression at both mRNA and protein levels in RTE cells, and that this effect was suppressed by rCC16 in a dose-dependent manner (Figure 2) at concentrations compatible to those detected *in vivo*,[43] suggesting the physiological significance of our rCC16 proteins.

NF-κB is one of the key transcription factors activated by LPS, and it has been implicated in regulating genes of the inflammatory cascade.[30] Activation of the NF-κB pathway is also associated with airway inflammation such as COPD, and suppression of this pathway has been shown to attenuate airway inflammations.[52,53] On the other hand, the promoter of MMP-9 gene contains a highly conserved motif that matches the NF-κB p65 binding element, and inhibition of NF-κB blocks MMP-9 up-regulation.[54] Here we show that level of MMP-9 in LPS-treated RTE cells was significantly reduced by the NF-κB inhibitor PDTC (supplemental Figure 3), suggesting a direct role of NF-κB pathway in MMP-9 expression. To explore the molecular mechanisms of rCC16 inhibition of LPS-induced MMP-9 expression, we examined the effect of rCC16 on LPS-induced NF-κB activation by using reporter gene assays and EMSA analysis. Our results showed that LPS could induce transcriptional activation of NF-κB and this effect was suppressed together with the formation of NF-κB-DNA complexes by rCC16 in a concentration-dependent manner (Figure 3). These data together indicate that rCC16 can inhibit LPS-induced NF-κB activation and its binding of gene promoters.

Next, we performed Western blotting analysis to determine whether rCC16 can block NF-κB activation through interruption of its signaling pathways. Both NF-κB translocation-dependent[55,56] and NF-κB phosphorylation-dependent[33] pathways have been implicated in the activation of NF-κB. It is well established that the subunit p50/p65 complex of NF-κB is generally sequestered by its inhibitor IκBα in the cytosol.[57] Upon stimulation, IκBα is phosphorylated, ubiquitinated, and degraded to release NF-κB/p65 which

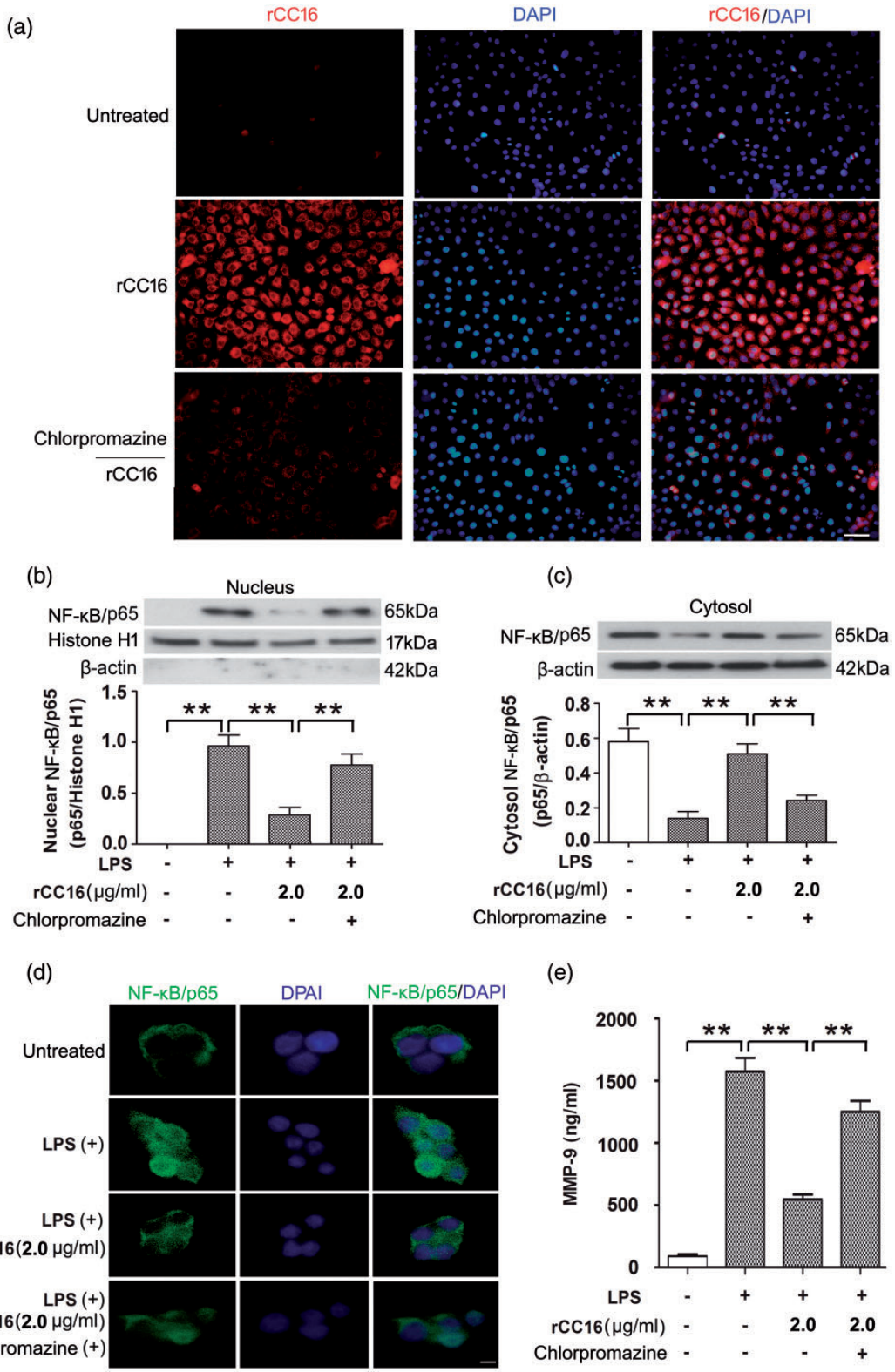

Figure 7 rCC16 enters RTE cells via clathrin-mediated endocytosis. (a) Chlorpromazine impedes uptake of rCC16 via clathrin-mediated endocytosis. RTE cells preincubated with chlorpromazine (30 mM; 30 min) or vehicles were exposed to rCC16 (2.0 μg/mL; 30 min) or PBS controls, immune-labeled with a mouse anti-His antibody for His-tagged rCC16 (red), and exposed to DAPI for nuclei (blue). Scale bar, 25 μm. (b, c) Chlorpromazine restores NF-κB nuclear translocation in rCC16-treated RTE cells. RTE cells treated as described in (a) were exposed to LPS at 0.1 μg/mL for 1 h and cytoplasmic and nuclear distributions of NF-κB/p65 were determined by Western blotting together with β-actin and Histone H1 as internal controls, respectively. The absence of detectable β-actin in the nucleus fraction indicated the absence of nuclear protein contaminations from the cytosolic fractions. Note the chlorpromazine blockage of rCC16 inhibitory effect on LPS-induced nuclear translocation of NF-κB/p65. (d) Immunofluorescence images show the subcellular distributions of NF-κB/p65 (green) with DAPI nuclear staining (blue) in RTE cells treated with or without LPS, rCC16, and chlorpromazine. Scale bar, 100 μm. (e) Chlorpromazine promotes release of MMP-9 in rCC16-treated RTE cells. Cell culture media collected from RTE cells as described in (b) were assessed for MMP-9 levels by ELISA assays. Note the chlorpromazine blockage of rCC16 inhibitory effect on LPS-stimulated MMP-9 secretion. All data are presented as the mean ± SD (n = 3) of three independent experiments. $^{**}p < 0.01$ indicates significant difference between groups as shown. (A color version of this figure is available in the online journal.)

then translocates to the nucleus to activate target genes. In addition, transcriptional activity of nuclear NF-κB is also regulated by post-translational modifications,[58] for instance, phosphorylation of its p65 subunit at Ser276[59,60] through the p38-MAPK signaling pathways.[61] Here we have demonstrated that rCC16 inhibits LPS-induced phosphorylation and degradation of IκBα (Figure 5), and translocation of NF-κB/p65 subunit from the cytosol into the nuclear fractions without affecting its total protein levels (Figure 4(a)). There is evidence that LPS induces the phosphorylation of p38 MAPK,[62] and that p38 MAPK activates NF-κB via phosphorylation of its p65 subunit at Ser276 during mitogen- and stress-activated protein kinases (MSKs) activations.[63] Additionally, LPS has been shown to phosphorylate NF-κB p65 at Ser276[64,65] which in turn regulates the transcriptional activity of NF-κB.[66,67] In line with these reports, we found that rCC16 inhibits LPS-induced phosphorylation of p65 subunit of NF-κB at Ser276 (Figure 6(a)), and that LPS-induced phosphorylation of p38 MAPK was markedly suppressed by rCC16 pretreatment in a concentration-dependent manner (Figure 6(b)).

Our observation that CC16 attenuates LPS-induced NF-κB activation through inhibiting IκBα phosphorylation and nucleus translocation of NF-κB would suggest that the translocation-dependent pathway plays a leading role in the RTE cells. This is consistent with the notion of this pathway as the first step for NF-κB signaling.[33] Our findings that rCC16 also inhibits LPS-induced phosphorylation of p38 MAPK and p65 subunit of NF-κB at Ser276 (Figure 6(a)) indicate that the p38 MAPK-dependent pathway is also operational in RTE cells. It appears that the two pathways work sequentially in facilitating transcriptional activities of NF-κB but our data here could not differentiate the pathways as both were inhibited by rCC16. There is no interaction between p65 and CC16 found in a previous study which attempted to define CC16-interacting proteins in NF-κB pathways.[68] Similarly, it is unclear if there is an upstream site that CC16 could impact. Nevertheless, our findings together suggest that rCC16 suppresses LPS-induced NF-κB activation by down-regulating both of its translocation- and phosphorylation-dependent pathways in RTE cells.

CC16 is synthesized primarily by non-ciliated bronchiolar epithelial cells, i.e. the Clara cells. It passively diffuses into plasma across the bronchoalveolar–blood barrier from the airways.[69] In accord, no endogenous expression of CC16 proteins was detected in the RTE cells in this study (supplemental Figure 2). To explore the route of rCC16 entry to RTE cells, we used chlorpromazine to block the formation of clathrin-coated pits at the plasma membrane in clathrin-mediated endocytosis. Our immunofluorescence staining assay showed that chlorpromazine inhibited the uptake of rCC16 by RTE cells (Figure 7(a)). Further Western blotting and ELISA analysis confirmed that chlorpromazine blockage of cellular rCC16 uptake significantly abolished rCC16 inhibition of LPS-induced nuclear translocation of NF-κB/p65 and down-stream MMP-9 expression (Figure 7(b), (c), and (e)). These findings suggest that rCC16 functions to inhibit MMP-9 expression in RTE cells through clathrin-mediated endocytosis.

Induction of CC16 expression by gene transfection has been shown to inhibit IL-1β induced IL-8 expression in bronchial epithelial BEAS-2B cells by suppressing the phosphorylation of IkBα and the transcriptional activity of NF-κB.[68] Our new observation was that rCC16 suppresses MMP-9 expression in LPS-stimulated RTE cells via clathrin-mediated endocytosis and inactivates both NF-κB and p38 MAPK-dependent signaling pathways. Although CC16 from different sources was used in these two studies, they all revealed the same mechanism that NF-κB pathway is involved in CC16's anti-inflammation role.

Studies currently under way in our laboratory are investigating the possible role of rCC16 in different cells of inflammatory association, including human airway epithelial cells. Further studies on the role of CC16 in airway inflammatory diseases and applications of rCC16 to its cellular and animal models could lead to the development of novel therapeutic strategies in the management of COPD-like disorders.

AUTHORS' CONTRIBUTIONS

YCD conceived and designed the experiments; MP, HLW, and YJ performed the experiments; DWC and JYX analyzed the data; CPZ, ZHL, XRZ, and XYH contributed reagents/materials/analysis tools; MP and J-ZB wrote the manuscript.

ACKNOWLEDGEMENTS

We thank Dr Min Yang and Kouhong Sun (Zoonbio Biotechnology Co. Ltd, Nanjing, China) for their technical assistance with HPLC and EMSA analysis. This work was supported by the National Natural Science Foundation of China (81200032), the scientific and technological projects of Shanxi Provincial Health Department (2011029), the Youth Science and Technology Fund of Shanxi Medical University (02201120), the Youth Science and Technology Fund of the First Hospital of Shanxi Medical University (YQ1102), and Outstanding Graduate Innovation Project of Shanxi Province (20123063).

CONFLICT OF INTEREST

The authors declare that there is no conflict of interest. The study sponsor had no role in the study design, in the collection, analysis, and interpretation of data, in the writing of the report, or in the decision to submit the paper for publication.

REFERENCES

1. Chen LC, Zhang Z, Myers AC, Huang SK. Cutting edge: altered pulmonary eosinophilic inflammation in mice deficient for Clara cell secretory 10-kDa protein. *J Immunol* 2001;**167**:3025–28
2. Nord M, Lag M, Cassel TN, Randmark M, Becher R, Barnes HJ, Schwarze PE, Gustafsson JA, Lund J. Regulation of CCSP (PCB-BP/uteroglobin) expression in primary cultures of lung cells: involvement of C/EBP. *DNA Cell Biol* 1998;**17**:481–92
3. Singh G, Katyal SL, Brown WE, Kennedy AL, Singh U, Wong-Chong ML. Clara cell 10 kDa protein (CC10): comparison of structure and function to uteroglobin. *Biochim Biophys Acta* 1990;**1039**:348–55
4. Dierynck I, Bernard A, Roels H, De Ley M. The human Clara cell protein: biochemical and biological characterisation of a natural immunosuppressor. *Mult Scler* 1996;**1**:385–7

5. Pilette C, Godding V, Kiss R, Delos M, Verbeken E, Decaestecker C, De Paepe K, Vaerman JP, Decramer M, Sibille Y. Reduced epithelial expression of secretory component in small airways correlates with airflow obstruction in chronic obstructive pulmonary disease. *Am J Respir Crit Care Med* 2001;**163**:185–94
6. Tsoumakidou M, Bouloukaki I, Thimaki K, Tzanakis N, Siafakas NM. Innate immunity proteins in chronic obstructive pulmonary disease and idiopathic pulmonary fibrosis. *Exp Lung Res* 2010;**36**:373–80
7. Shijubo N, Itoh Y, Yamaguchi T, Imada A, Hirasawa M, Yamada T, Kawai T, Abe S. Clara cell protein-positive epithelial cells are reduced in small airways of asthmatics. *Am J Respir Crit Care Med* 1999;**160**:930–3
8. Snyder JC, Reynolds SD, Hollingsworth JW, Li Z, Kaminski N, Stripp BR. Clara cells attenuate the inflammatory response through regulation of macrophage behavior. *Am J Respir Cell Mol Biol* 2010;**42**:161–71
9. Taggart CC, Greene CM, Carroll TP, O'Neill SJ, McElvaney NG. Elastolytic proteases: inflammation resolution and dysregulation in chronic infective lung disease. *Am J Respir Crit Care Med* 2005;**171**:1070–6
10. Vandooren J, Van den Steen PE, Opdenakker G. Biochemistry and molecular biology of gelatinase B or matrix metalloproteinase-9 (MMP-9): the next decade. *Crit Rev Biochem Mol Biol* 2013;**48**:222–72
11. Boschetto P, Quintavalle S, Zeni E, Leprotti S, Potena A, Ballerin L, Papi A, Palladini G, Luisetti M, Annovazzi L, Iadarola P, De Rosa E, Fabbri LM, Mapp CE. Association between markers of emphysema and more severe chronic obstructive pulmonary disease. *Thorax* 2006;**61**:1037–42
12. Russell RE, Culpitt SV, DeMatos C, Donnelly L, Smith M, Wiggins J, Barnes PJ. Release and activity of matrix metalloproteinase-9 and tissue inhibitor of metalloproteinase-1 by alveolar macrophages from patients with chronic obstructive pulmonary disease. *Am J Respir Cell Mol Biol* 2002;**26**:602–9
13. Mercer PF, Shute JK, Bhowmik A, Donaldson GC, Wedzicha JA, Warner JA. MMP-9, TIMP-1 and inflammatory cells in sputum from COPD patients during exacerbation. *Respir Res* 2005;**6**:151
14. Lemjabbar H, Gosset P, Lamblin C, Tillie I, Hartmann D, Wallaert B, Tonnel AB, Lafuma C. Contribution of 92 kDa gelatinase/type IV collagenase in bronchial inflammation during status asthmaticus. *Am J Respir Crit Care Med* 1999;**159**:1298–1307
15. Li YT, He B, Wang YZ, Wang J. Effects of intratracheal administration of nuclear factor-kappaB decoy oligodeoxynucleotides on long-term cigarette smoke-induced lung inflammation and pathology in mice. *Respir Res* 2009;**10**:79
16. Yang L, Yao CS, Wu ZY, Xuan LL, Bai JY, Cheng GF, Lin M, Wen MC, Hou Q. Effects of dihydroxy-stilbene compound Vam3 on airway inflammation, expression of ICAM-1, activities of NF-kappaB and MMP-9 in asthmatic mice. *Yao Xue Xue Bao* 2010;**45**:1503–8
17. Lee IT, Yang CM. Inflammatory signalings involved in airway and pulmonary diseases. *Mediators Inflamm* 2013;**2013**:791231
18. Yan C, Wang H, Aggarwal B, Boyd DD. A novel homologous recombination system to study 92 kDa type IV collagenase transcription demonstrates that the NF-kappaB motif drives the transition from a repressed to an activated state of gene expression. *FASEB J* 2004;**18**:540–1
19. Mendes Sdos S, Candi A, Vansteenbrugge M, Pignon MR, Bult H, Boudjeltia KZ, Munaut C, Raes M. Microarray analyses of the effects of NF-kappaB or PI3K pathway inhibitors on the LPS-induced gene expression profile in RAW264.7 cells: synergistic effects of rapamycin on LPS-induced MMP9-overexpression. *Cell Signal* 2009;**21**:1109–22
20. Pang M, Du Y, Jiang Y, Liu Z, Zhang C, Chen LC, Wang H. Gene-cloning, prokaryotic expression and purification of rat Clara cell secretory protein (Chinese). *J Environ Health* 2013;**30**:290–4
21. Hu L, Liu Y, Cheng S. Simultaneous determination of six analytes by HPLC-UV for high throughput analysis in permeability assessment. *J Chromatogr Sci* 2011;**49**:124–8
22. Yang M, Wu J, Xu X, Jin Y, Guo Y, Chen J. A new lignan from the Jian-er syrup and its content determination by RP-HPLC. *J Pharm Biomed Anal* 2006;**41**:662–6
23. Chen S, Wu Z. The method of determination of phospholipase A2 in fluids and tissues samples (Chinese). *Acad J Second Mil Med Univ* 1989;**10**:254–6
24. Meng X, Kou C, Li C, Shi J, Yu Q, Ming J, Yu Y. Association between serum phospholipase A2 activity and schizophrenia (Chinese). *J Jilin Univ (Med Ed)* 2007;**33**:723–5
25. Zheng B1, Zhou J, Geng Q, Dong Q. A preliminary study on the origin of human lung adenocarcinoma stem cells from lung bonchioalveolar stem cells. *Zhongguo Fei Ai Za Zhi* 2008;**11**:759–64
26. Jorens PG, Sibille Y, Goulding NJ, van Overveld FJ, Herman AG, Bossaert L, De Backer WA, Lauwerys R, Flower RJ, Bernard A. Potential role of Clara cell protein, an endogenous phospholipase A2 inhibitor, in acute lung injury. *Eur Respir J* 1995;**8**:1647–53
27. Nogaki T, Asano K, Furuta A, Kanai K, Suzaki I, Kanei A, Suzaki H. Enhancement of clara cell 10-kD protein (CC10) production from nasal epithelial cells by fexofenadine hydrochloride. *Asian Pac J Allergy Immunol* 2012;**30**:139–45
28. Martin TR. Recognition of bacterial endotoxin in the lungs. *Am J Respir Cell Mol Biol* 2000;**23**:128–32
29. Li YQ, Yan JP, Xu WL, Wang H, Xia YJ, Wang HJ, Zhu YY, Huang XJ. ADAM17 mediates MMP-9 expression in lung epithelial cells. *PLoS One* 2013;**8**:e51701
30. Kim HJ, Jeong JS, Kim SR, Park SY, Chae HJ, Lee YC. Inhibition of endoplasmic reticulum stress alleviates lipopolysaccharide-induced lung inflammation through modulation of NF-kappaB/HIF-1alpha signaling pathway. *Sci Rep* 2013;**3**:1142
31. Raulo SM, Sorsa T, Tervahartiala T, Pirila E, Maisi P. MMP-9 as a marker of inflammation in tracheal epithelial lining fluid (TELF) and in bronchoalveolar fluid (BALF) of COPD horses. *Equine Vet J* 2001;**33**:128–36
32. Uwe S. Anti-inflammatory interventions of NF-kappaB signaling: potential applications and risks. *Biochem Pharmacol* 2008;**75**:1567–79
33. Oeckinghaus A, Hayden MS, Ghosh S. Crosstalk in NF-kappaB signaling pathways. *Nat Immunol* 2011;**12**:695–708
34. Tam WF, Sen R. IkappaB family members function by different mechanisms. *J Biol Chem* 2001;**276**:7701–4
35. Reber L, Vermeulen L, Haegeman G, Frossard N. Ser276 phosphorylation of NF-kB p65 by MSK1 controls SCF expression in inflammation. *PLoS One* 2009;**4**:e4393
36. Le Roy C, Wrana JL. Clathrin- and non-clathrin-mediated endocytic regulation of cell signalling. *Nat Rev Mol Cell Biol* 2005;**6**:112–26
37. Doherty GJ, McMahon HT. Mechanisms of endocytosis. *Annu Rev Biochem* 2009;**78**:857–902
38. Wang LH, Rothberg KG, Anderson RG. Mis-assembly of clathrin lattices on endosomes reveals a regulatory switch for coated pit formation. *J Cell Biol* 1993;**123**:1107–17
39. Irander K, Palm JP, Borres MP, Ghafouri B. Clara cell protein in nasal lavage fluid and nasal nitric oxide – biomarkers with anti-inflammatory properties in allergic rhinitis. *Clin Mol Allergy* 2012;**10**:4
40. Benson M, Jansson L, Adner M, Luts A, Uddman R, Cardell LO. Gene profiling reveals decreased expression of uteroglobin and other anti-inflammatory genes in nasal fluid cells from patients with intermittent allergic rhinitis. *Clin Exp Allergy* 2005;**35**:473–8
41. Arsalane K, Broeckaert F, Knoops B, Wiedig M, Toubeau G, Bernard A. Clara cell specific protein (CC16) expression after acute lung inflammation induced by intratracheal lipopolysaccharide administration. *Am J Respir Crit Care Med* 2000;**161**:1624–30
42. Lensmar C, Nord M, Gudmundsson GH, Roquet A, Andersson O, Jörnvall H, Eklund A, Grunewald J, Agerberth B. Decreased pulmonary levels of the anti-inflammatory Clara cell 16 kDa protein after induction of airway inflammation in asthmatics. *Cell Mol Life Sci* 2000;**57**:976–81
43. Hermans C, Bernard A. Lung epithelium specific proteins: characteristics and potential applications as markers. *Am J Respir Crit Care Med* 1999;**159**:646–78
44. Won TB, Quan SH, Rhee CS, Min YG, Lee CH. Expression of uteroglobin in a murine model of allergic rhinitis. *Acta Otolaryngol* 2007;Suppl: 83–89

45. Vlahos R, Wark PA, Anderson GP, Bozinovski S. Glucocorticosteroids differentially regulate MMP-9 and neutrophil elastase in COPD. *PLoS One* 2012;**7**:e33277
46. Halade GV, Jin YF, Lindsey ML. Matrix metalloproteinase (MMP)-9: a proximal biomarker for cardiac remodeling and a distal biomarker for inflammation. *Pharmacol Ther* 2013;**139**:32–40
47. Russell RE, Thorley A, Culpitt SV, Dodd S, Donnelly LE, Demattos C, Fitzgerald M, Barnes PJ. Alveolar macrophage-mediated elastolysis: roles of matrix metalloproteinases, cysteine, and serine proteases. *Am J Physiol Lung Cell Mol Physiol* 2002;**283**:L867–873
48. Jouneau S, Khorasani N, Souza DEP, Macedo P, Zhu J, Bhavsar PK, Chung KF. EMMPRIN (CD147) regulation of MMP-9 in bronchial epithelial cells in COPD. *Respirology* 2011;**16**:705–12
49. Tacon CE, Wiehler S, Holden NS, Newton R, Proud D, Leigh R. Human rhinovirus infection up-regulates MMP-9 production in airway epithelial cells via NF-κB. *Am J Respir Cell Mol Biol* 2010;**43**:201–9
50. Perera WR, Hurst JR, Wilkinson TM, Sapsford RJ, Mullerova H, Donaldson GC, Wedzicha JA. Inflammatory changes, recovery and recurrence at COPD exacerbation. *Eur Respir J* 2007;**29**:527–34
51. Abe N, Osanai T, Fujiwara T, Kameda K, Matsunaga T, Okumura K. C-reactive protein-induced upregulation of extracellular matrix metalloproteinase inducer in macrophages: inhibitory effect of fluvastatin. *Life Sci* 2006;**78**:1021–8
52. Hayden MS, Ghosh S. Shared principles in NF-kappaB signaling. *Cell* 2008;**132**:344–62
53. Agusti A, Morla M, Sauleda J, Saus C, Busquets X. NF-kappaB activation and iNOS upregulation in skeletal muscle of patients with COPD and low body weight. *Thorax* 2004;**59**:483–7
54. Zhang K, Zhang Y, Cheng YJ, Lu L. Effects of Shenqi Bufei Tang on expressions of NF-kappaB, MMP-9 and TIMP-1 in airway remodeling of COPD rat model with lung-Qi deficiency syndrome. *Zhongguo Zhong Yao Za Zhi* 2008;**33**:2129–32
55. Wang Z, Leng Y, Tsai LK, Leeds P, Chuang DM. Valproic acid attenuates blood-brain barrier disruption in a rat model of transient focal cerebral ischemia: the roles of HDAC and MMP-9 inhibition. *J Cereb Blood Flow Metab* 2011;**31**:52–57
56. Karin M, Ben-Neriah Y. Phosphorylation meets ubiquitination: the control of NF-[kappa]B activity. *Annu Rev Immunol* 2000;**18**:621–63
57. Schmitz ML, Baeuerle PA. The p65 subunit is responsible for the strong transcription activating potential of NF-kappa B. *EMBO J* 1991;**10**:3805–17
58. Hayden MS, Ghosh S. Signaling to NF-kappaB. *Genes Dev* 2004;**18**:2195–2224
59. Zhong H, SuYang H, Erdjument-Bromage H, Tempst P, Ghosh S. The transcriptional activity of NF-kappaB is regulated by the IkappaB-associated PKAc subunit through a cyclic AMP-independent mechanism. *Cell* 1997;**89**:413–24
60. Zhong H, May MJ, Jimi E, Ghosh S. The phosphorylation status of nuclear NF-kappa B determines its association with CBP/p300 or HDAC-1. *Mol Cell* 2002;**9**:625–36
61. Kefaloyianni E, Gaitanaki C, Beis I. ERK1/2 and p38-MAPK signalling pathways, through MSK1, are involved in NF-kappaB transactivation during oxidative stress in skeletal myoblasts. *Cell Signal* 2006;**18**:2238–51
62. Chen LF, Greene WC. Shaping the nuclear action of NF-kappaB. *Nat Rev Mol Cell Biol* 2004;**5**:392–401
63. Zhao D, Ding R, Mao Y, Wang L, Zhang Z, Ma X. Heparin rescues sepsis-associated acute lung injury and lethality through the suppression of inflammatory responses. *Inflammation* 2012;**35**:1825–32
64. Gilmore TD. Introduction to NF-kappaB: players, pathways, perspectives. *Oncogene* 2006;**25**:6680–4
65. Kim WI, Ryu HJ, Kim JE, Seo CH, Lee BC, Choi IG, Kang TC. Differential nuclear factor-kappa B phosphorylation induced by lipopolysaccharide in the hippocampus of P2X7 receptor knockout mouse. *Neurol Res* 2013;**35**:369–81
66. Chen LY, Pan WW, Chen M, Li JD, Liu W, Chen G, Huang S, Papadimos TJ, Pan ZK. Synergistic induction of inflammation by bacterial products lipopolysaccharide and fMLP: an important microbial pathogenic mechanism. *J Immunol* 2009;**182**:2518–24
67. Furusawa J, Funakoshi-Tago M, Tago K, Mashino T, Inoue H, Sonoda Y, Kasahara T. Licochalcone A significantly suppresses LPS signaling pathway through the inhibition of NF-kappaB p65 phosphorylation at serine 276. *Cell Signal* 2009;**21**:778–85
68. Long XB, Hu S, Wang N, Zhen HT, Cui YH, Liu Z. Clara cell 10-kDa protein gene transfection inhibits NF-kappaB activity in airway epithelial cells. *PLoS One* 2012;**7**:e35960
69. Gioldassi XM, Papadimitriou H, Mikraki V, Karamanos NK. Clara cell secretory protein: determination of serum levels by an enzyme immunoassay and its importance as an indicator of bronchial asthma in children. *J Pharm Biomed Anal* 2004;**34**:823–6

(Received August 22, 2014, Accepted December 12, 2014)